University of Nebraska - Lincoln

# DigitalCommons@University of Nebraska - Lincoln

Papers in the Earth and Atmospheric Sciences

Earth and Atmospheric Sciences, Department of

2015

# Diagenetic incorporation of Sr into aragonitic bivalve shells: implications for chronostratigraphic and palaeoenvironmental interpretations

Maria C. Marcano
*University of Michigan*

Tracy D. Frank
*University of Nebraska at Lincoln,* tfrank2@unl.edu

Samuel B. Mukasa
*University of New Hampshire*

Kyger C. Lohmann
*University of Michigan*

Marco Taviani
*ISMAR*

Follow this and additional works at: https://digitalcommons.unl.edu/geosciencefacpub

Part of the Earth Sciences Commons

## ORIGINAL RESEARCH ARTICLE

# Diagenetic incorporation of Sr into aragonitic bivalve shells: implications for chronostratigraphic and palaeoenvironmental interpretations

MARIA C. MARCANO*, TRACY D. FRANK†, SAMUEL B. MUKASA‡, KYGER C LOHMANN* and MARCO TAVIANI§,¶

*Department of Earth and Environmental Sciences, University of Michigan, 2534 C. C. Little Building, 1100 North University Ave., Ann Arbor, MI 48109-1005, USA

†Department of Earth and Atmospheric Sciences, University of Nebraska-Lincoln, 214 Bessey Hall, Lincoln, NE 68588-0340, USA

‡College of Engineering and Physical Sciences, University of New Hampshire, Kingsbury Hall W289, 33 Academic Way, Durham, NH 03824-3591, USA

§Istituto di Scienze Marine (ISMAR) – CNR, Via Gobetti 101, 40129, Bologna Italy

¶Biology Department, Woods Hole Oceanographic Institution, 266 Woods Hole Road, Woods Hole, MA 02543, USA

## ABSTRACT

Aragonite is easily altered during diagenesis, therefore presumed pristine when present. In effect, beyond polymorphic transformation to calcite, alteration paths of aragonite remain poorly understood despite heavy reliance on such material to produce palaeoenvironmental and chronostratigraphic interpretations. Previous work on core material from Southern McMurdo Sound, Antarctica, showed that unlike their calcitic counterparts, seemingly unaltered aragonite shell fragments invariably produced older than expected $^{87}Sr/^{86}Sr$ ages. In this study, we pursued additional analyses of these aragonite shells and of the porewater of the core to understand this discrepancy. Aragonite mineralogy was reconfirmed and elemental mapping of shell fragments revealed growth lines within the middle layer suggestive of good preservation. The outer layer, however, showed anomalously high Sr concentrations (average $4·5 \pm 0·6$ mole% $SrCO_3$; *ca* 25 mmol $mol^{-1}$ Sr/Ca) and was depleted in $^{18}O$ and $^{13}C$ compared to the middle layer, both features inconsistent with pristine material. The $\delta^{18}O$ values and Sr concentrations of the porewater were used to model outer layer compositions reasonably well. Coincidentally, porewater Sr isotope composition was in general agreement with the age model of the core only at the aragonite-bearing interval suggesting that Sr-isotopic disequilibrium between porewater and the carbonates was the rule rather than the exception in the core. The Sr isotope compositions of the aragonite shells are most likely the result of early diagenesis as suggested by the inconsistent O and C isotope compositions between shell layers and the anomalously high Sr concentrations. We conclude that knowledge of Sr concentration and distribution in shells is critical to determine the viability of Sr stratigraphy and the scale at which it may be applied. Reliance on traditional indicators of lack of alteration, such as cathodoluminescence, Mn-Fe concentration, and the presence of labile mineralogies to assert chronostratigraphic and palaeoenvironmental questions may produce erroneous conclusions due to obscurely altered material.

## INTRODUCTION

The $^{87}Sr/^{86}Sr$ ratios of unaltered marine biogenic carbonates are routinely compared to the well-established secular variation of Sr isotopic composition of sea water (Hess *et al.*, 1986; Howarth & McArthur, 1997; McArthur *et al.*, 2001) to provide chronostratigraphic control. Because the residence time of Sr in sea water is considerably longer

than the mixing time of the oceans and because Sr is not fractionated by near-surface physicochemical processes, Sr isotopic composition of sea water at any one time is homogeneous and thus reflects the balance between global rock distribution, rock-type proportion and weathering intensity (Graustein, 1989; Faure & Mensing, 2005). Given that carbonate secreting organisms do not fractionate Sr when they incorporate it in their skeletons, the $^{87}Sr/^{86}Sr$ ratio of the open oceanic sea water can be reconstructed through geological time using unaltered biogenic carbonate material. In this context, well-preserved samples can also be used to estimate Sr sources and to model past mixing and weathering rates, although these relationships are not straightforward and numerous components of the climate system appear to play different roles of variable importance at different points in time. For example, modelling suggests that most of the increase in sea water $^{87}Sr/^{86}Sr$ since the mid Pliocene can be explained solely by the relative rise in phyllosilicates weathering prompted by global cooling (Li *et al.*, 2007), while Kashiwagi *et al.* (2008) conclude that sea water $^{87}Sr/^{86}Sr$ cannot be used as a direct proxy for silicate weathering and atmospheric $CO_2$ decrease during the Cenozoic.

Strontium stratigraphy is not applicable to intervals where plateaus in the secular variation of radiogenic Sr prevent time discrimination, or to areas where large freshwater inputs can deviate the biogenic carbonate signal from the global averages (Ingram & Depaolo, 1993; Israelson & Buchardt, 1999; Sessa *et al.*, 2012). However, Sr isotope composition from well-preserved biogenic carbonates of neritic and bathyal marine environments, where conventional chronostratigraphic methods are problematic due to frequent hiatuses and reworking, can be helpful in establishing time constraints. That was an immediate analytical target offered by the several macro-fossil-bearing intervals of core AND-2A recovered by the ANDRILL (ANtarctic Geological DRILLing) program during its second field campaign (i.e., the Southern McMurdo Sound (SMS) project) during the austral summer of 2007 (Fig. 1).

The multinational ANDRILL program is a joint effort to drill the margin of Antarctica in search of Cenozoic stratigraphic records to study variation in ice sheets and obtain a better understanding of polar climate evolution (Harwood *et al.*, 2005, 2006, 2009). Specific goals for the SMS project included: (i) improve chronostratigraphic control; (ii) document melt-water discharge events from the Dry Valleys of the TransAntarctic Mountains and (iii) evaluate the persistence of polar conditions in Antarctica over the past 15 Myr. Extracting this critical information on continental evolution from marginal sediments, however, is not without complications. The biogenic-rich

intervals of the core were sampled in part to assess the aforementioned objectives using Sr and O isotopes.

The Sr isotope compositions of pristine marine samples are considered to accurately reflect precipitation age. Previous analyses of venerid and pectinid shells from the macrofossil-rich intervals of core AND-2A (Taviani *et al.*, 2009) were suggestive of minimal to no diagenetic alteration. The Sr isotope compositions of unaltered calcitic pectinid fragments provided additional chronostratigraphic control to the core (Acton *et al.*, 2008). In contrast with calcite fragments, Sr isotope compositions of the aragonitic venerid shells were lower than expected in all samples resulting in older than reasonable Sr-isotopic ages, while Sr concentrations of the aragonite shells were higher than those observed in modern bivalves (Marcano *et al.*, 2009).

Given the significance of chronostratigraphic and palaeoenvironmental interpretations reliant on the Sr content of carbonate samples, and considering that the aragonite anomalous Sr isotope compositions of samples from core AND-2A were not unequivocally explained using basic isotopic mass balance calculations, these samples were further explored here using more detailed techniques and evaluated against new Sr data from the porewater of the core. Unlike biogenic carbonates, interstitial fluids in AND-2A appeared to be highly modified as suggested by initial chemical analyses of porewater and fracture filling cements (Gui, 2009; Frank & Gui, 2010). Here, the Sr concentrations and isotope compositions of AND-2A porewater were explored to better understand the results from shell studies and more broadly assess the use of $^{87}Sr/^{86}Sr$ as a definite chronostratigraphic indicator from carbonates whose alteration has been ruled out using limited criteria.

## Previous work: Sr compositions of biogenic material from other Antarctic cores

Several studies from previous Antarctic coring efforts produced Sr isotope ages consistent with independently determined age estimates. The Sr isotope ratios measured in aragonitic bivalves recovered from DSDP Site 270 in the southeastern portion of the Ross Sea and from CIROS-1, off Ferrar Glacier in McMurdo Sound (Barrera, 1989), produced ages consistent with biostratigraphic estimates. Similarly, several aragonitic bivalve samples from the Cape Roberts Project (CRP) cores, drilled about 65 km north of CIROS-1, produced Sr ages consistent with Ar isotope ages and diatom-based biostratigraphy (Lavelle, 1998, 2000, 2001). Most of these ages (8 out of 11) remain valid even after the age model of CRP-2/2A was astrochronologically adjusted across the Oligocene-Miocene boundary (Naish *et al.*, 2008).
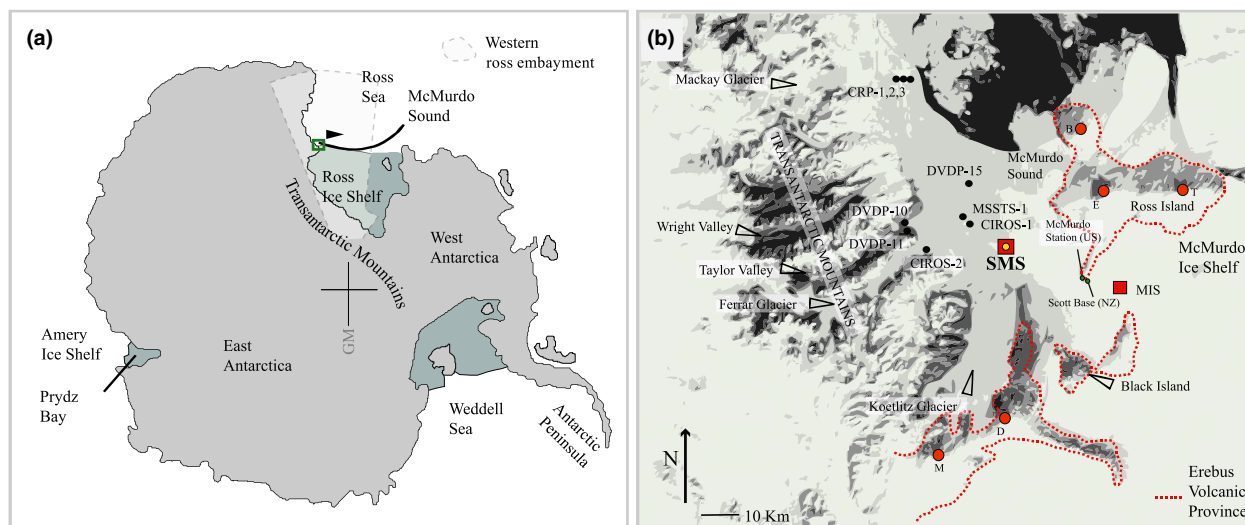
**Fig. 1.** Location map. (A) McMurdo Sound at the edge of the Ross Ice Shelf, Antarctica. (B) ANDRILL SMS (Southern McMurdo Sound) and MIS (McMurdo Ice Shelf) drill-holes location in Southern McMurdo Sound (squares). CRP – Cape Roberts Project; DVDP – Dry Valley Drilling Project; MSSTS – McMurdo Sound Sediment and Tectonic Study; CIROS – Cenozoic Investigations of the Ross Sea. Dotted line demarks the Erebus volcanic province; B – Mount Bird; E – Mount Erebus; T – Mount Terror; M – Mount Morning; D – Mount Discovery. Modified from Harwood *et al.* (2005).

Other studies have produced mixed results, with Sr isotope compositions inconsistent with stratigraphic age. For example, shells from the first ANDRILL core recovered in McMurdo Sound (AND-1B, MIS – McMurdo Ice Sheet Project, Naish *et al.*, 2007) yielded somewhat ambiguous Sr isotope ages (Wilson *et al.*, 2007). Within the uncertainty of shell fragment identification, the bivalves appeared to be consistently associated with lower than expected Sr isotope values, while other macrofossils (mainly foraminifera and cirripeda) produced ages closer to the age model of the core. Mineralogy of bivalve fragments was not specified, and therefore it is uncertain whether the older ages were associated with aragonitic bivalves only, as was the case in the AND-2A core. Wilson *et al.* (2007) concluded that the most likely cause of the age discrepancy was contamination by matrix sediments. However, results continued to be equivocal after several cycles of HCl etching of the shell fragments, suggesting that ambiguous Sr isotope compositions were probably intrinsic to the shell and not a product of contamination. Partial equilibration with porewaters was proposed by Wilson *et al.* (2007) as an alternate cause of the anomalous isotopic compositions, but this hypothesis was not tested.

The Sr isotope compositions of bivalve shells positively identified as aragonite reported from ODP Site 739 in Prydz Bay, Antarctica, also produced unexpected ages (Thierstein *et al.*, 1991). In this case, the Sr isotope ages were younger (latest Early Oligocene-earliest Miocene) than the aragonite shell-bearing stratigraphic units (uppermost Eocene-lowermost Oligocene). Porewaters from the same depths as the shell-bearing diamictites were analysed for Sr concentration and isotopic composition. The Sr concentrations were between 1·5 and 2 times higher than that of modern sea water, and Sr isotope ratios were among the most radiogenic ever recorded by the ODP and DSDP. Thierstein *et al.* (1991) calculated that measured aragonite Sr isotope compositions would require either a 90% contribution from freshwater to the depositional fluid or 10% to 17% post-depositional incorporation of Sr from the extant porewater. They also calculated that porewater compositions could be reasonably derived from altered continental detritus.

Approaches used in the studies mentioned above were not consistent. For example, identification, description and criteria to rule out alteration or transport varied widely. This may in part explain the disparity of results. In any case, the apparent pristine aragonite of the macrofossil shells remained puzzling and required further investigation.

## MATERIALS AND METHODS

Previous analyses to identify and discriminate alteration effects on these and other selected macrofossil fragments are described in Marcano *et al.* (2009). Here, we focus on AND-2A venerid aragonitic fragments recovered between 429·28 m and 430·51 m below seafloor (mbsf) identified

as in-house samples number 9, 10, 11-1, 15-2 and 15-3. These fragments belong to a venerid bivalve recently shown to be a species new to Science and described by Beu & Taviani (2014) as *Retrotapes andrillorum*. The outer and middle layer could be clearly recognized in most fragments. Marcano *et al.* (2009) sampled the outer and middle layers separately for chemical analyses, but relatively large sample sizes were required for conventional powder X-ray diffraction technique. Results could not account for the presence of small, localized alteration products or resolve differences among layers.

Powder X-ray microdiffraction (PXRD) was used in this study to reconfirm mineralogy without sample homogenization. PXRD patterns were collected on a Riga-ku R-Axis Spider diffractometer with an imaging plate detector using graphite monochromated Cu-Kα radiation (1·5406 Å) at ambient temperature. Whole fragments of venerid shell exhibiting both outer and middle layers were used. The sample was mounted on a cryoloop with par-atone N oil for analysis, and the diffractogram obtained from sections of samples where both layers occupied approximate equal volumes. To avoid preferred orientation, images were collected for 5 min while rotating the sample about the φ-axis at $10°s^{-1}$ and oscillating ω between 120° and 180° at $1°s^{-1}$, with ψ set at 45° (see additional online material for an illustration of the sample orientation). These were integrated with a 0·05° step size with the AreaMax2 software package.

The aragonite shell fragments were further sampled from the outer and middle layer to measure oxygen and carbon isotope composition and supplement previous published values (Marcano *et al.*, 2009). Separates were roasted in vacuo, at 200°C, to eliminate volatile contaminants. Oxygen and carbon isotope ratios were determined using an automated Kiel IV device coupled to a triple-collector gas source Finnigan MAT 253 isotope-ratio mass spectrometer and reported against the VPDB (Vienna PeeDee Belemnite) standard. Standard deviations for both carbon and oxygen are equal to or better than 0·1‰.

Electron microprobe elemental mapping was done to localize areas of anomalous Sr concentration in the shell. The X-ray mapping was carried out on a cross section of a shell fragment (sample 10) using wavelength-dispersive (WLD) spectrometry in a Cameca SX-100 electron probe microanalyser (EPMA). Data were collected from three spectrometers with a detection limit of 270 p.p.m. To avoid precision limitations imposed by the analytical time necessary to quantify the entire Sr map, concentrations were measured along three transects, each 270 μm in length along the cross-section of the fragment. Beam diameter was adjusted to 5, 2 and <0·5 μm with each step size varying from 5 to 2 μm, producing a total of 245 measurements. Secondary electron images were also acquired from the mapped areas and for the rest of the shell fragments, which showed cleaned, unaltered prismatic material.

Porewater chemistry was measured on-ice and discussed elsewhere (Panter *et al.*, 2008). Here, Sr concentrations of porewaters were determined on a Perkin Elmer Optima 3300 DV inductively coupled plasma-optical emission spectrometer (ICP-OES) using 10-point calibration curves. One High-Purity® standard solution (Trace Metals in Drinking Water) and one in-house standard indicated that accuracy of the chemical analyses was ±5% RSD or better for Sr and Ca.

The Sr concentrations were used to determine initial porewater sample size for Sr isotope determinations. After complete porewater evaporation 2·5N HCl was added to the residues. Strontium was then separated using column chromatography (Mukasa *et al.*, 1991). Samples were dried to a solid, treated with a drop of 14N $HNO_3$, re-dried, and loaded on a single Re filament. The Sr was loaded with 0·1 vol% $H_3PO_4$ and $TaClO_4$ solution. The $^{87}Sr/^{86}Sr$ measurements were done on a VG Sector multi-collector thermal ionization mass spectrometer (TIMS). The Sr isotope composition was corrected for mass fractionation using $^{86}Sr/^{88}Sr = 0·1194$. The repeated analyses of NBS-987 standard ($n = 3$) gave an average $^{87}Sr/^{86}Sr = 0·710252 \pm 10 \times 10^{-6}$. Total blanks averaged 0·35 ng for Sr, which are negligible (Table 1).

All analyses described above were carried out in the Chemistry Department and the Earth and Environmental Sciences Department of the University of Michigan in Ann Arbor, Michigan.

## RESULTS

Powder patterns from the PXRD patterns were processed in Jade Plus3 to calculate peak positions and intensities. The Jade software package developed by Materials Data Inc. (MDI) supports and provides access to comprehensive XRD databases such as the Powder Diffraction Files (PDF 2 and 4), produced by the International Center for Diffraction Data (ICDD). The suggested match was exclusively aragonite, with both layers contributing equally to the result.

Electron microprobe elemental mapping identified areas of anomalous Sr concentration in the shell (Fig. 2; see additional online material for a complete list of the results). The backscattered electron (BSE) image suggested that the mineralogy of the middle and outer layers of the venerid fragment was uniform (i.e., no high-Sr alteration phase). Instead of occurring in isolated phases, Sr appeared highly and evenly concentrated in the prismatic outer layer of the shell and along well-defined lines in the crystallographic homogeneous middle layer. Samples

**Table 1.** Sr and Ca concentrations and Sr isotope compositions of AND-2A porewater.

| In-house ID | | Depth (mbsf) | p.p.m.* | | mmol mol$^{-1}$ | $^{87}$Sr/$^{86}$Sr | Error |
|---|---|---|---|---|---|---|---|
| | | | Ca | Sr | Sr/Ca | | |
| PW | 1 | 9·67 to 9·72 | 590·707 | 10·014 | 7·75 | 0·70807 | 1·1 × 10$^{-5}$ |
| PW | 2-1 | 30·09 to 30·15 | 477·209 | 4·172 | 4·00 | 0·70987 | 1·0 × 10$^{-5}$ |
| PW | 3-1 | 37·41 to 37·46 | 342·930 | 3·041 | 4·06 | 0·70996 | 1·0 × 10$^{-5}$ |
| PW | 4 | 43·72 to 43·77 | 187·016 | 1·624 | 3·97 | 0·71003 | 1·1 × 10$^{-5}$ |
| PW | 5 | 51·30 to 51·35 | 174·668 | 2·092 | 5·48 | 0·71018 | 1·7 × 10$^{-5}$ |
| PW | 6 | 57·21 to 57·26 | 181·939 | 1·495 | 3·76 | 0·71012 | 1·5 × 10$^{-5}$ |
| PW | 7 | 62·66 to 62·71 | 289·175 | 5·026 | 7·95 | — | — |
| PW | 8 | 81·03 to 81·08 | — | — | — | 0·71022 | 1·0 × 10$^{-5}$ |
| PW | 9 | 91·97 to 93·03 | — | — | — | 0·71017 | 1·0 × 10$^{-5}$ |
| PW | 10-1 | 92·97 to 93·03 | 268·230 | 3·465 | 5·91 | 0·71009 | 1·3 × 10$^{-5}$ |
| PW | 11 | 116·22 to 116·27 | 805·600 | 10·752 | 6·11 | 0·71001 | 1·0 × 10$^{-5}$ |
| PW | 12 | 155·76 to 155·81 | — | — | — | 0·70963 | 1·0 × 10$^{-5}$ |
| PW | 13 | 235·66 to 235·76 | — | — | — | 0·70889 | 1·0 × 10$^{-5}$ |
| PW | 14-1 | 336·18 to 336·28 | 1973·065 | 31·512 | 7·31 | 0·70872 | 1·2 × 10$^{-5}$ |
| PW | 15 | 353·53 to 353·63 | 2017·073 | 35·442 | 8·04 | 0·70870 | 1·1 × 10$^{-5}$ |
| PW | 16 | 545·01 to 545·11 | 1604·868 | 49·121 | 14·00 | 0·70842 | 1·0 × 10$^{-5}$ |
| PW | 17 | 619·35 to 619·45 | 3154·357 | 61·999 | 8·99 | 0·70855 | 1·0 × 10$^{-5}$ |
| PW | 18 | 779·69 to 779·79 | 4136·569 | 84·366 | 9·33 | 0·70692 | 1·0 × 10$^{-5}$ |
| PW | 19 | 109·84 to 809·94 | — | — | — | 0·70711 | 1·0 × 10$^{-5}$ |
| PW | 20 | 963·44 to 963·54 | 3558·582 | 81·286 | 10·45 | 0·70802 | 1·0 × 10$^{-5}$ |

*Accuracy better than ±5% for Sr and Ca concentrations.

strictly within the outer prismatic layer averaged 2·3 ± 0·4 wt% Sr (4·5 ± 0·6 mole% SrCO$_3$) ($n$ = 15, error is ± 2σ), a concentration about five times that of the middle layer lines (0·5 ± 0·2 wt% Sr or 1·0 ± 0·4 mole% SrCO$_3$, $n$ = 43, error is ±2σ). These high-Sr lines in turn had about twice the background Sr concentration of the middle layer (0·3 ± 0·1wt%, 0·5 ± 0·2 mole% SrCO$_3$, $n$ = 184, error is ±2σ).

The Sr$^{2+}$ concentration of porewater varied from a minimum of 1·5 to 84·4 p.p.m.; while Ca$^{2+}$ varied from 175 to 4,137 p.p.m. (Table 1). Behaviour of Sr$^{2+}$ and Ca$^{2+}$ downcore was very similar decreasing in the upper 60 m to their respective minima and increasing thereafter. The Sr$^{2+}$ and Ca$^{2+}$ concentrations diverged between *ca* 336 mbsf and 545 mbsf, where Ca$^{2+}$ decreased while Sr continued to increase. In the uppermost 60 m of the core, Sr$^{2+}$/Ca$^{2+}$ varied from 7·75 mmol mol$^{-1}$ at *ca* 10 mbsf to its minimum (*ca* 4 mmol mol$^{-1}$) and back to *ca* 8 mmol mol$^{-1}$. From about 93 mbsf to the bottom of the core, porewater Sr$^{2+}$/Ca$^{2+}$ steadily increased to a maximum of *ca* 10 mmol mol$^{-1}$, with only one sample off the trend at *ca* 545 mbsf (Fig. 3).

Porewater Sr isotope compositions in the upper *ca* 200 m of the core showed large deviations from the age model of the core (Fig. 4; Table 1). Close to the top of the core, porewater $^{87}$Sr/$^{86}$Sr was well below modern sea water values (0·70807 ± 15). From this depth to *ca* 235 mbsf, Sr isotope compositions increased to their

maximum (0·71022 ± 15 at 73·18 mbsf) and then decreased to values close to those predicted by the age model of the core (0·70889 ± 15 at 235·71 mbsf) where they remained relatively stable to a depth of *ca* 620 mbsf. Porewater $^{87}$Sr/$^{86}$Sr dropped to its lowest values at 779·74 mbsf (0·70692 ± 15) and finally increased to the deepest porewater measured at *ca* 960 mbsf to values still below those corresponding to the age model (0·70802 ± 15).

Supplementary stable isotopes samples produced average δ$^{18}$O of −5·7‰ from the outer layer and −2·1‰ from the middle layer, while δ$^{13}$C averages are −4·5‰ and −0·2‰ from outer and middle layer samples, respectively (Fig. 5). Aragonite δ$^{18}$O and δ$^{13}$C are highly correlated.

# INTERPRETATION AND DISCUSSION

## Strontium in aragonite bivalve shells

Thin bivalve shells are considered by some to be among the least reliable materials to preserve sea water Sr isotope ratios (Smalley *et al.*, 1994). However, because aragonite is easily altered during early diagenesis (Bathurst, 1975; Brand & Veizer, 1980), bivalve shells that retain their original aragonite mineralogy are presumed pristine and thus expected to preserve their original chemical composition. Lack of pervasive alteration of AND-2A venerid
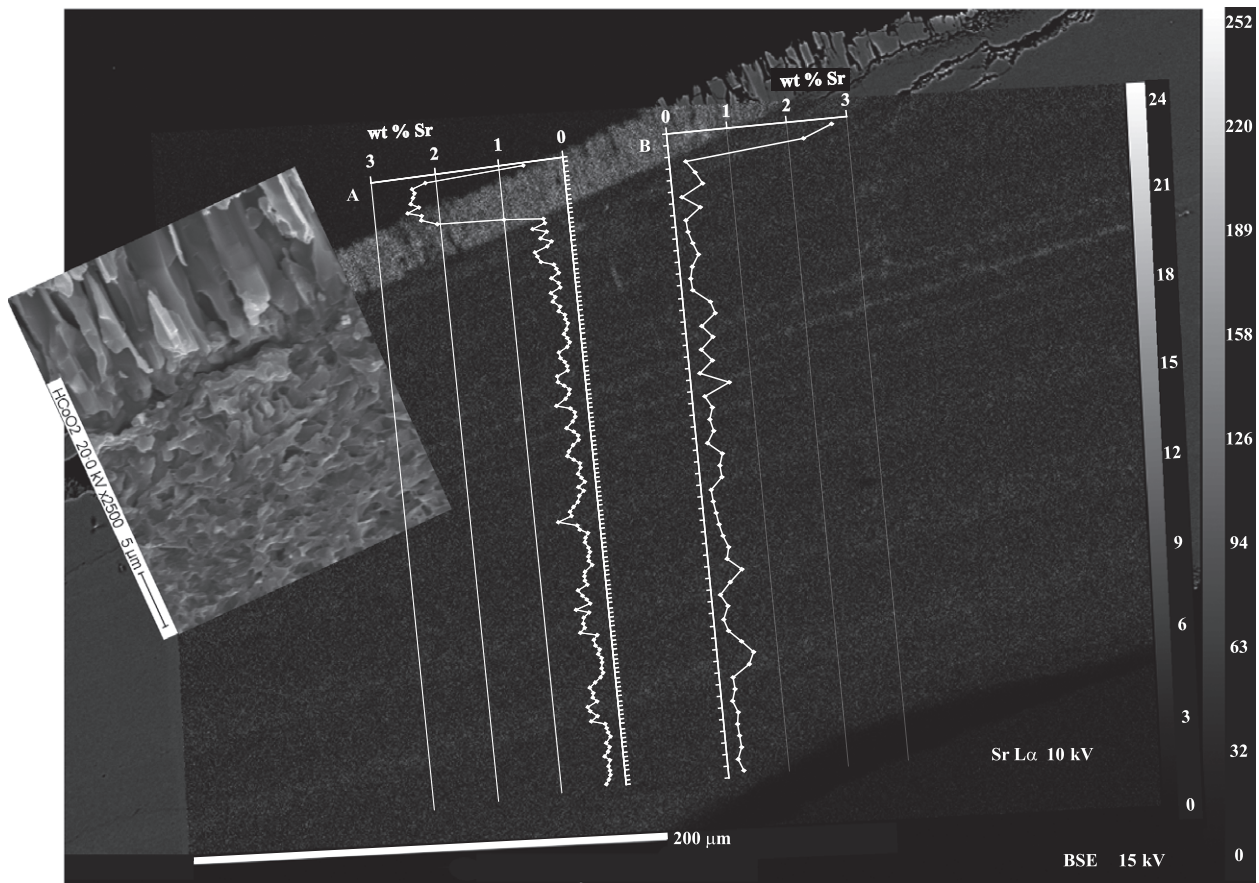
**Fig. 2.** Sr compositional map over background BSE image (visible at the edges) of in-house sample number 10 from 430·49 to 430·51 mbsf. Scale bar applies to both images. Two of the three measured compositional profiles are superimposed on the elemental map. Measurement locations are shown as points along the abscissa. Profile A: beam diameter 2 μm, sample spacing 2 μm. Profile B: beam diameter 0·5 μm, sample spacing 5 μm. The representative SEM image overlay in the upper-left has a different scale.

shells was previously inferred based on the absence of cathodoluminescence, high Sr and low Fe-Mn concentrations (Marcano *et al.*, 2009). In the present study, the mineralogy of both layers of the same bivalve samples was reconfirmed by microdiffraction.

The Sr concentration contrast observed within the middle layer of the venerid fragments from AND-2A (Fig. 2) may be reasonably explained as the result of Sr concentration fluctuating in response to seasonal changes, which either influence Sr availability or the physiology of the bivalve that in turns controls Sr distribution. For example, in a number of previous studies, Sr incorporation into bivalves has been variably correlated to temperature, and also to growth rate and maturity (Dodd, 1965; Stecher *et al.*, 1996; Hart & Blusztajn, 1998; Dutton *et al.*, 2002; Gillikin *et al.*, 2005; Freitas *et al.*, 2006; Surge & Walker, 2006; Elliot *et al.*, 2009). However, no unique relationship has been established, and as suggested by some, controls on Sr incorporation into bivalve shells

may even be species specific (Gillikin *et al.*, 2005; Bailey & Lear, 2006). Regardless of the cause, controlling factors of Sr incorporation into skeletal aragonite vary as the carbonate is incrementally added to the shell, thereby producing a record of growth such as that observed in Figure 2.

However, suggestive of primary precipitation the observed growth lines are, their Sr concentrations are anomalously high compared to modern bivalves, in particular those of the outer layer. Modern molluscs in general discriminate against skeletal Sr incorporation, and their Sr content is usually less than 0·77 mole% $SrCO_3$ (Kinsman, 1969; Veizer, 1983; Morse & MacKenzie, 1990). Modern aragonite cements, on the other hand, contain between 1·2 mole% $SrCO_3$ and 2·3 mole% $SrCO_3$, although inorganic aragonite with up to 14 mole % $SrCO_3$ has been reported from hot spring deposits (Morse & MacKenzie, 1990). Unusually high Sr contents in AND-2A bivalves suggest that recrystallization of the
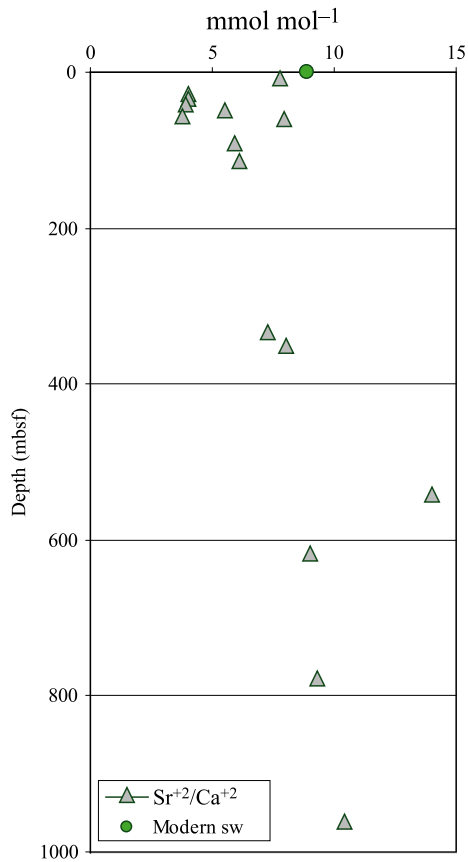
**Fig. 3.** Sr²⁺/Ca²⁺ variation with depth. Below *ca* 93 mbsf, Sr²⁺/Ca²⁺ increases moderately to the core bottom with one sample at *ca* 545 mbsf off the trend.



**Fig. 4.** Sr isotope compositions of porewater (blue diamonds) and previously analysed carbonate samples (Marcano *et al.*, 2009). Circles: pectinid samples (calcite). Triangles: venerid samples (aragonite). Green symbols are samples with no clear indications of alteration; yellow symbols are samples marginally altered; red symbols are clearly altered samples. Black open circles: AND-2A age model data. Overall age range is indicated by the grey vertical band. Modern sea water $^{87}Sr/^{86}Sr$ value indicated by blue circle at depth 0 mbsf. The large and predominant discrepancy between the Sr isotope values of the samples and the porewater is indicative of disequilibrium and suggestive of allochtonous fluids. Limited concurrences are better interpreted as coincidental.

outer layer, a neomorphic process in which the mineral persists after reaction, probably occurred (Folk, 1965; Bathurst, 1975). Therefore, the prismatic structure observed in the Sr-rich outer layer of AND-2A venerid samples, observed also in modern aragonite bivalves, is not sufficient evidence to reject the potential presence of a secondary carbonate because the crystal form can persist through mineralogical stabilization. Crystal structure preservation occurs when diagenetic reactions take place through migrating solution films, which allows chemical changes to occur at the crystal boundaries without developing porosity (Kinsman, 1969; Maliva *et al.*, 2000).

Authigenic aragonite has not been described in AND-2A, but general conditions favourable for carbonate precipitation from the porewater (i.e., very high alkalinity) exist throughout the length of the core. Also, Wada & Okada (1989) described aragonite cements at a variety of depths in the CIROS-1 core, which was drilled less than 30 km away from the locality of this study (Fig. 1). Detailed description of the porewater chemistry and the diagenetic conditions are published elsewhere (Panter
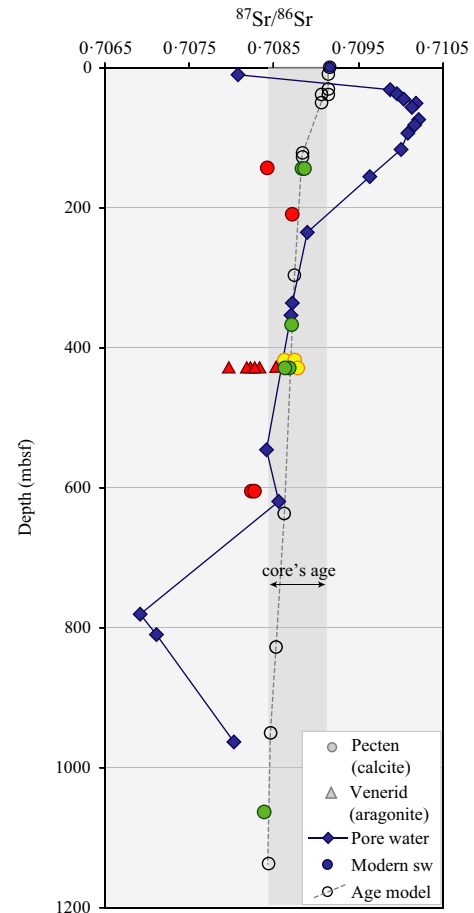
*et al.*, 2008; Frank & Gui, 2010). Knowledge of the specific saturation state of the pore fluids, however, is not useful given the disequilibrium between porewater and shell aragonite shown by Sr isotopes and the localized nature of the recrystallization process.

As pointed out by Marcano *et al.* (2009), calculated non-thermodynamic Sr partition coefficients ($K_{Sr}$) for aragonite between 0·4 and 2 are necessary to obtain the measured Sr concentrations in AND-2A shells if these were precipitating from normal modern sea water. A simple non-thermodynamic calculation using a Sr partition
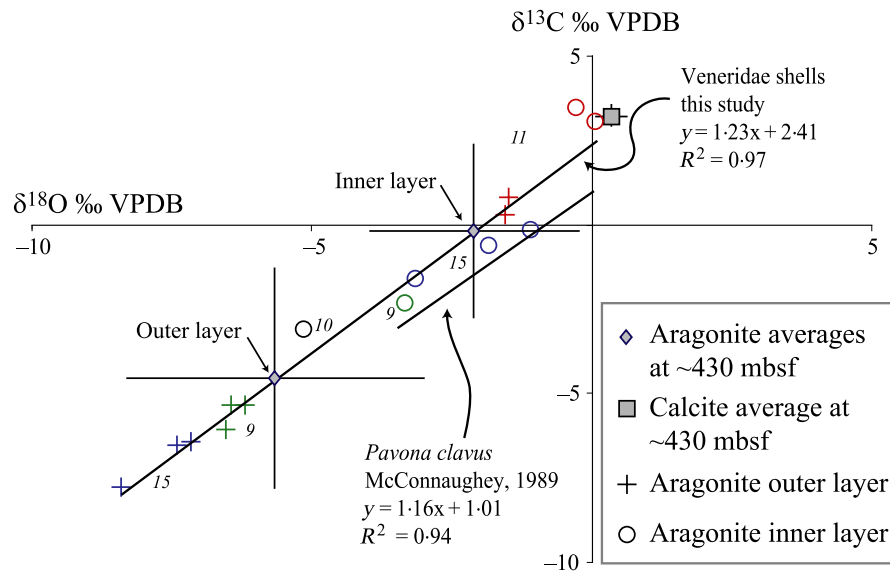
**Fig. 5.** Oxygen and carbon isotope compositions of AND-2A bivalve samples. Open squares: pectinid samples (calcite). Open circles and crosses: middle and outer layer samples, respectively (aragonite). In-house sample identification number in italics: 15 blue symbols, 11 red symbols, 10 black symbols, 9 green symbols. Error of averages is 2σ. Linear fit was calculated to all aragonite data. Tropical coral *Pavona clavus* data from McConnaughey (1989a,b) plotted for comparison.

coefficient of 1·13 (calculated by interpolating to 24°C the values of the distribution coefficient calculated by Kinsman & Holland (1969) at 16°C and 80°C), suggests that the Sr concentrations of aragonite cement precipitating from modern porewater at the level of interest, where $Sr^{2+}/Ca^{2+}$ could potentially vary between 8 mmol mol$^{-1}$ and 14 mmol mol$^{-1}$ (Fig. 3), should be between 9 mmol mol$^{-1}$ and 16 mmol mol$^{-1}$. Although narrower, this range is in good agreement with the 4 to 18 mmol mol$^{-1}$ Sr/Ca measured in bulk samples of the AND-2A aragonite shell fragments (Marcano *et al.*, 2009). There are limitations associated with this calculation, in particular when considering the high ionic strength of AND-2A porewater. Nevertheless, higher aragonite Sr concentrations can certainly be modelled using the Sr in porewater instead of sea water.

Inorganic precipitation of aragonite has been used to calculate the temperature-dependent partition of Sr in aragonite. These experiments have produced relatively consistent $K_{Sr}$ values close to 1 for temperatures <100°C (Kinsman & Holland, 1969; Dietzel *et al.*, 2003; Gaetani & Cohen, 2006). All of these calculations imply that the Sr/Ca in aragonite should be very close to the $Sr^{2+}/Ca^{2+}$ in the fluid from which it precipitates. However, Bathurst (1975) in analysing the calculations of Kinsman & Holland (1969), noted the large uncertainties involved (>3500 p.p.m. variation in Sr concentration of inorganic aragonite precipitating from a known fluid at a fixed temperature). Moreover, Gaetani & Cohen (2006) pointed

out the large discrepancy between the values based on experimental precipitation and their theoretical calculations. Their theoretical approaches return considerably lower distribution coefficients, which are directly instead of inversely correlated to temperature. The authors suggest that aragonites that conform to a partition coefficient close to 1 are actually strongly enriched in Sr relative to the expected equilibrium concentrations, which should be between 0·5 mmol mol$^{-1}$ and 1 mmol mol$^{-1}$ for temperatures from 15 to 75°C. This disagreement suggests that the incorporation of Sr in aragonite is a complex process not yet fully understood and probably more so in biogenic aragonite.

## Alteration scenarios

Although recrystallization without mineralogical change probably occurred, a satisfactory diagenetic process to explain it and further physical evidence of its occurrence are both difficult to produce. The original aragonitic outer shell material must have been dissolved to once more precipitate as aragonite. Carbonate cement compositions are in part controlled by the mineralogy of the particles present in the sediment (Walter, 1986), and although in this case cementation *sensu stricto* did not occur, it illustrates the plausibility of primary mineralogy controlling diagenetic phases. Unless conditions that inhibit calcite precipitation exist, the more thermodynamically stable calcite crystals will tend to precipitate from

fluids saturated with respect to aragonite. Aragonite and high-magnesian calcite, the common skeletal carbonate materials to precipitate in shallow environments, are in metastable equilibrium with sea water and will tend to recrystallize to calcite in the early diagenetic environment (inversion of Folk, 1965; polymorphic transformation of Bathurst, 1975). Although the presence of ions in the pore fluids influences mineral equilibria, and the free energies of formation of pure aragonite and pure calcite are close enough that small changes in the fluid can impact their equilibria (Bathurst, 1975; Morse & MacKenzie, 1990), it is difficult to explain fluid changes across migrating films so that aragonite is dissolved and reprecipitated as the film advances. Even if kinetic processes supersede thermodynamic controls of solution-precipitation (as is common in natural carbonates), it is unclear why diagenetic stabilization should increase Sr concentration. Diagnostic physical products of recrystallization without mineralogical change were absent in petrographic and SEM preliminary observations of AND-2A samples.

Studies on solid-state diffusion of $Cd^{2+}$ on calcite demonstrated that this mechanism is capable of incorporating cations into the bulk of the solid and likely to play a role in the uptake of trace metals by other mineral groups as well (Stipp et al., 1992). Although diffusion in carbonate minerals has been regarded relevant only at high temperature and pressure, it may be an important factor in standard conditions, highlighting the potential uncertainties associated to techniques based on the assumption of minerals functioning as perfectly closed system (Stipp et al., 1998).

AND-2A aragonite shells are characterized by low Mn and Fe concentrations, an otherwise good indicator for lack of extensive diagenetic alteration. However, the low Mn and Fe concentrations may be a reflection of their absence in the diagenetic environment, probably an indication of conditions sufficiently oxidizing to prevent reduction of oxides and hydroxides. Abundant iron-rich oxidizing phases and the near absence of organic matter support this possibility. In addition, Mn and Fe share structural affinity to the trigonal calcite, not the orthogonal aragonite. This alone may have prevented their incorporation into the secondary carbonate, even if present in the sediment after the death of the bivalves. Slow recrystallization may have also prevented inclusion of Mn and Fe in aragonite (Morse & MacKenzie, 1990).

If Sr concentrations of the aragonite shell can be achieved as described, and recrystallization occurred and was limited largely to the outer layer, crystal structure may have played a role in promoting chemical changes. Solubility can be influenced by crystal properties and mineral structure differences typically exist between bivalve layers and also between growth lines within a single layer. According to Walter & Morse (1985), thermodynamically more stable carbonate phases can in some cases dissolve faster than less stable ones due to differences in microstructural complexity. Consequently, the original contrast in crystalline structure is likely to translate into a stability gradient between the bivalve layers, which will result in selective or localized diagenetic stabilization.

Because the alteration scenarios discussed above are based mainly on the excessive Sr concentration of the outer layer and its contrast with the middle layers, which are not by themselves diagenetic indicators, it is necessary to examine them as potential primary features. While some modern aragonite bivalves show Sr enrichment in the outer layer (Shirai et al., 2014), not all do. Elliot et al. (2009) obtained similar average Sr/Ca from different layers of modern Tridacna gigas specimens, although the middle layers showed higher variability. Neither average nor variability differences could be distinguished between the Sr/Ca ratios from the prismatic outer layer and the crossed-lamellar middle layer of Mercenaria campechiensis from the Gulf Coast of Florida (salinity between 19 and 36), although Sr concentration behaviour with respect to $\delta^{18}O$ differed between layers (Surge & Walker, 2006). Takesue et al. (2008) found significant differences in several cation-to-Ca ratios as a function of the aragonite crystal structure in the estuarine bivalve Corbula amurensis, with the notable exceptions of Sr and Na. The shell used to perform the latter analysis grew in waters with a maximum salinity of 28·5. Interestingly, Foster et al. (2009) studying the marine cold water bivalve Arctica islandica found significant Sr/Ca differences between samples from the axis of maximum growth and those from transects parallel to it, as well as between and within aragonite from the umbo and the outer shell layer. They concluded that changes in shell architecture were a likely candidate to control Sr incorporation through Sr distribution coefficient changes associated with differences in crystal growth. Their analyses were not designed to sample different crystal structures, but the differences they observed keep open the possibility of structure mediated Sr incorporation in some aragonitic bivalves, perhaps an indirect consequence of contrasting growth rates. Still, in the studies mentioned above, Sr/Ca in the aragonite shells remains below ca 3 mmol $mol^{-1}$, while the outer layer of AND-2A sample 10, for example, averages 25 mmol $mol^{-1}$. This mechanism is most likely unable to concentrate Sr at the levels found in this outer layer.

In summary, a primary origin of aragonitic shells from AND-2A may be suggested by the presence of primary growth lines in the shells and the lack of Sr-isotopic equilibrium between the shells and the ambient porewater. The difficulties associated with physically documenting

and chemically explaining potential diagenetic changes in the outer layer of AND-2A *Retrotapes* and the uncertainties in the partition coefficient of Sr in aragonite could be used to further the argument of lack of alteration. Nevertheless, the extreme Sr concentration of the outer layer is difficult to reconcile with precipitation by a living bivalve and also with the fresh water input that would be required to explain the more negative $\delta^{18}O$ measured in the outer layer, which will be discussed later. A primary origin is therefore unlikely.

## Porewater Sr isotope compositions

Excluding a relatively small deviation at 545·06 mbsf, porewater Sr isotope compositions are within the age model of the core and range between *ca* 336 and 620 mbsf (Fig. 4). This section includes the aragonite-bearing interval at *ca* 430 mbsf. At all other depths porewater Sr isotope compositions diverge substantially from the age model of the core. Unlike porewater, Sr-isotopic ratios of unaltered calcite shell fragments were in agreement with the age model in the aragonite-bearing interval (366·83 mbsf) and also above and below (144·05 mbsf and 1063·72 mbsf; Marcano *et al.*, 2009). Although porewater may appear to have maintained its original Sr isotope composition at the aragonite-bearing level, this is probably not the case.

Carbonate Sr isotopes require high water-to-rock ratios (on the order of $10^3$) to equilibrate with fluids unless these are brines. In that case equilibration can occur at considerably lower water-to-rock ratios (*ca* 10), similar to those required to equilibrate oxygen during freshwater diagenesis (Banner & Hanson, 1990). AND-2A porewater is highly saline, increasing linearly at a rate of about 30 per 100 m depth and stabilizing below *ca* 500 mbsf to salinities between 150 and 200 in the practical salinity scale (Frank & Gui, 2010). Alkalinity is also high (maximum *ca* 55 meq kg$^{-1}$).

For brines in particular, appropriate chemical models to describe mineral solubility in subsurface conditions are lacking, and non-equilibrium processes are probably the norm (Morse & MacKenzie, 1990). Nevertheless, given the observed carbonate-porewater isotopic contrasts, the highly modified chemistry of AND-2A porewater and the age of the stratigraphic column, late modification or substitution of the porewater probably occurred in this area, which is located only a few tens of kilometres from the coast. Porewater compositions of the DSDP Sites 270 to 273 in the continental shelf of the Ross Sea, for example, are very different from AND-2A fluids. Maximum alkalinity reported is 25 meq kg$^{-1}$, although it remains mostly below 10 meq kg$^{-1}$, while salinity drops with depth from normal marine to *ca* 27 (Mann & Gieskes, 1975). They

also reported a slight Sr concentration increase downcore possibly associated with aragonite dissolution. Sr concentration in AND-2A decreases in the uppermost part of the core and begins to increase steadily below *ca* 120 mbsf. The unusual Sr isotopic composition of AND-2A porewater is highlighted by the Elderfield & Gieskes (1982) study, which summarized Sr concentration and isotopic composition trends from 37 DSDP holes with latitudinal distribution between 0·5° and 69·9° (Median = 31·53° lat). In contrast to AND-2A, overall porewater isotopic compositions in all analysed drill-holes decrease with depth from normal or close to normal modern marine values in the upper 10 mbsf, to a minimum of 0·70490. Strontium isotope compositions significantly greater than modern sea water were not measured in any of the more than 160 porewater data sets included in this study.

The extant porewater Sr isotope compositions appear not to be just the direct result of reactions with volcanic glass. Throughout AND-2A volcanic alteration products are found in close proximity to unaltered glass (Fielding *et al.*, 2008). Given the reactive nature of volcanic material, the presence of unaltered grains may in part indicate that some of the alteration products originated at the sedimentary source instead of the subsurface. The Sr isotope compositions of porewater are inadequate to explain the anomalous Sr isotope compositions in AND-2A aragonites and give support to a parautochtonous origin of the porewater. What is more, these observations highlight the potential for invalid interpretations if stabilization with the current porewater had occurred. In such a case, the Sr isotope composition of the water fortuitously matching the age model of the core would have not raised further suspicions about the integrity of the aragonite shells. Consequently, ruling out alteration using only basic criteria such as mineralogy, crystal structure, and Mn and Fe content may be misleading.

## Oxygen and Carbon isotopic compositions of aragonite bivalve shells

Calcite pectinids and aragonite venerids at *ca* 430 mbsf have contrasting oxygen and carbon isotope compositions (Fig. 5). While all measured shell calcites at *ca* 430 mbsf ($n = 3$) produced very similar $\delta^{18}O$ and $\delta^{13}C$ values, aragonites did not. Calculated equilibrium $\delta^{18}O$ values for aragonite (between $-10·3‰$ and $-11·0‰$) using the oxygen isotope composition of the porewater (about $-10‰$; Frank & Gui, 2010) and the borehole temperatures at the level of the aragonite-bearing interval (between 21°C and 24°C; Wonik *et al.*, 2008) are at least 2‰ lower than the lowest $\delta^{18}O$ measured in the venerid shell outer layer ($-8·4‰$) and up to 9·5‰ lower than the most positive

shell $\delta^{18}O$ value ($-1\cdot5\text{‰}$). These estimates were calculated using the Grossman & Ku (1986) corrected palaeotemperature equation, which is in good agreement with relationships based on theoretical estimates of water-aragonite oxygen fractionation at equilibrium (Kim *et al.*, 2007).

The modelled $\delta^{18}O$ values show variable levels of disequilibrium between the aragonitic shells and the porewater for the conditions of the core today. However, using lower temperatures, it is possible to replicate the measured aragonite $\delta^{18}O$ values. This scenario requires alteration to occur earlier in the burial history of the samples without further re-equilibration. In the upper 50 m of the core, temperatures increase from *ca* 0 to 5°C, while water $\delta^{18}O$ decreases from modern sea water values of *ca* $-1\text{‰}$ to about $-10\text{‰}$ (Wonik *et al.*, 2008; Frank & Gui, 2010). Aragonite $\delta^{18}O$ precipitating in this interval would have compositions between *ca* $+3\cdot5\text{‰}$ and $-6\text{‰}$. Under stable conditions with respect to temperature and porewater $\delta^{18}O$, maximum alteration could have occurred when the sample was *ca* 200 mbsf. This is a good indication that parts of the shell could have been subjected to early alteration. The moderate $Sr^{2+}/Ca^{2+}$ increase at depth (Fig. 3) suggests that dissolution of Sr-rich phases is occurring, although this normal diagenetic trend may not be locally dominant as appears to be the case at the aragonite-bearing interval.

The carbon isotope composition of the shell is a function of the isotopic composition of the bicarbonate from which it forms, which in turn reflects the incorporation of organic and inorganic carbon, as well as metabolic fractionation. Variations in carbon isotopic composition indicate, in part, changes in productivity that are a function of depth or microhabitat conditions (Grossman & Ku, 1986; Hoefs, 1997), and these are difficult to predict or estimate. Although metabolic $CO_2$ appears to have a limited influence on molluscan carbonate (McConnaughey & Gillikin, 2008; Beirne *et al.*, 2012), it is unlikely that C can be incorporated into biogenic carbonate exclusively reflecting hydrological conditions (i.e., without vital effects). The $\delta^{13}C$ difference between calcite and aragonite was argued to reflect in part contrasting life styles between the pectinid and venerid bivalves (Marcano *et al.*, 2009).

Considerable differences exist in both oxygen and carbon isotope values between outer and middle layers. Values in outer layers are more negative than those from corresponding middle layers. Bivalve shell layers are formed from different pallial fluid sources along different areas of the mantle (Moore, 1969; McConnaughey & Gillikin, 2008), and adjacent points from different layers do not necessarily form at the same time. This discrepancy may be exacerbated by rapid growth. Primary intra-shell

contrast in $\delta^{13}C$ is common, but intra-shell contrasts in $\delta^{18}O$, although reported (Elliot *et al.*, 2009), are normally absent (Surge & Walker, 2006). While $\delta^{18}O$ comparisons between layers in most studies are based on long, usually multiyear data from complete valves, the millimetre-sized fragments analysed here provide data from a single point and this may help explain the contrast. However, the $\delta^{18}O$ difference between the layers can be better explained as the product of localized alteration.

The high correlation between $\delta^{18}O$ and $\delta^{13}C$ values and its similarity with such relationships observed in corals (Gonzalez & Lohmann, 1985; McConnaughey, 1989a, b) could be argued to represent disequilibrium precipitation in contrast with the equilibrium fractionation that characterizes most modern molluscs (Epstein *et al.*, 1953; Grossman & Ku, 1986). A fairly good correlation between $\delta^{18}O$ and $\delta^{13}C$ values has been reported for the modern venerid *M. mercenaria* (Elliot *et al.*, 2003), and departures from established oxygen isotope equilibrium fractionation of aragonite exist in other clams (Carré *et al.*, 2005). These observations suggest that disequilibrium precipitation in aragonite bivalves is possible. Kinetic effects probably associated with periods of rapid growth are the main cause of disequilibrium and likely a consequence of the seasonal growth in bivalves. Although the similarity between the slopes of linear fits to the venerid data and to coral data is intriguing (Fig. 5), the possibility of primary precipitation out of equilibrium cannot be tested, and as was mentioned above, the more negative values of the outer layer are not explained using the primary precipitation argument. Thus, the high $\delta^{18}O - \delta^{13}C$ correlation remains unexplained.

## CONCLUSION

Previous work had shown that aragonite bivalve fragments recovered from ANDRILL AND-2A core in Southern McMurdo Sound, Antarctica, passed generally accepted criteria for unaltered aragonite and showed Sr concentration contrast along growth lines of the middle layer. The Sr concentrations in the outer layer, however, were anomalously high, and Sr isotope compositions of all subsamples were less radiogenic than expected (Marcano *et al.*, 2009). Within the uncertainties associated with the incorporation of Sr into aragonite, the observed high-Sr concentration of the shells was modelled here using AND-2A porewater. Alteration was also suggested by the persistent depletion in $^{18}O$ of the outer layers compared to the middle layers, and the successful calculation of shell isotopic values using core temperatures and porewater $\delta^{18}O$. The Sr isotope compositions of the porewater and the aragonite shells differed. AND-2A porewater was highly modified and in general disequilibrium

with the core carbonates. In addition, Sr isotope compositions of the porewater deviated from that of the Ross Sea shelf and from *ca* 160 other porewater compositions reported by Elderfield & Gieskes (1982). The Sr concentration at the levels reported here (i.e., Sr/Ca as high as 25 mmol mol$^{-1}$), although not easily explained chemically or supported petrographically as a product of alteration, is in strong disagreement with modern primary shell precipitation. The presence of aragonite with no visual indications and only partial evidence of chemical alteration have been also reported for other molluscs, mostly on the nacreous layer of inoceramids, ammonoids and gastropods (Dauphin *et al.*, 2007; Cochran *et al.*, 2010; Wierzbowski *et al.*, 2012). Together, these observations confirm that the anomalous Sr concentrations and isotope compositions observed in the aragonite bivalves of AND-2A, equally expressed along diachronous layers of the shell, are likely the result of early diagenesis. Changes may have been selective, affecting differently the distinct crystal structures of the shell, which are variably susceptible to alteration. Evaluating mineralogy, cathodoluminescence and abundance of minor elements typically associated with diagenesis (i.e., Mn, Fe) is not enough to rule out alteration in Cenozoic Antarctica biogenic aragonites. Knowledge of Sr concentration and distribution in the shell is critical to determining the viability of Sr stratigraphy and the scale at which it may be applicable.

## ACKNOWLEDGEMENTS

## References

**Acton, G.**, **Crampton, J.**, **Di Vincenzo, G.**, **Fielding, C.G.**, **Florindo, F.**, **Hannah, M.J.**, **Harwood, D.M.**, **Ishman, S.E.**, **Johnson, K.**, **Jovane, L.**, **Levy, R.H.**, **Lum, B.**, **Marcano, M.C.**, **Mukasa, S.B.**, **Ohneiser, C.**, **Olney, M.**, **Riesselman, C.**, **Sagnotti, L.**, **Stefano, C.**, **Strada, E.**, **Taviani, M.**, **Tuzzi, E.**, **Verosub, K.L.**, **Wilson, G.S.** and **Zattin, M.** (2008) Preliminary Integrated chronostratigraphy of the AND-2A core, ANDRILL Southern McMurdo Sound Project Antarctica. In: Studies from the ANDRILL, Southern McMurdo Sound Project, Antarctica (Eds D.M. Harwood, F. Florindo, F. Talarico and R.H. Levy), Terra Antarct., **15**, 212–220.

**Bailey, T.R.** and **Lear, C.H.** (2006) Testing the effect of carbonate saturation of the Sr/Ca of biogenic aragonite: a case study from the River Ehen, Cumbria, UK. Geochem. Geophys. Geosyst., **7**, Q03019, doi:10.1029/2005GC001084.

**Banner, J.L.** and **Hanson, G.N.** (1990) Calculation of simultaneous isotopic and trace element variations during water-rock interaction with applications to carbonate diagenesis. Geochim. Cosmochim. Acta, **54**, 3123–3137.

**Barrera, E.** (1989) Strontium isotope ages. In: Antarctic Cenozoic History from the CIROS-1 drillhole, McMurdo Sound, Antarctica (Ed. B. , P. J), DSIR Bull., **245**, 151–152.

**Bathurst, R.G.C.** (1975) Carbonate Sediments and Their Diagenesis. Elsevier, Amsterdam, 593 pp.

**Beirne, E.C.**, **Wanamaker, A.L., Jr** and **Feindel, S.C.** (2012) Experimental validation of environmental controls on the $\delta^{13}$C of *Arctica islandica* (ocean quahog) shell carbonate. Geochim. Cosmochim. Acta, **84**, 395–409.

**Beu, A.** and **Taviani, M.** (2014) Early Miocene Mollusca from McMurdo Sound, Antarctica (ANDRILL 2A drill core), with a review of Antarctic Oligocene and Neogene Pectinidae (Bivalvia). Palaeontology, **57**, 299–342.

**Brand, U.** and **Veizer, J.** (1980) Chemical diagenesis of a multicomponent carbonate system 1: trace elements. J. Sed. Petrol., **50**, 1219–1236.

**Carré, M.**, **Bentaleb, I.**, **Blamart, D.**, **Ogle, N.**, **Cardenas, F.**, **Zevallos, S.**, **Kalin, R.M.**, **Ortilieb, L.** and **Fontugne, M.** (2005) Stable isotopes and sclerochronology of the bivalve *Mesodesma donacium*: potential application to Peruvian paleoceanographic reconstructions. Palaeogeogr. Palaeoclimatol. Palaeoecol., **228**, 4–25.

**Cochran, J.K.**, **Kallenberg, K.**, **Landman, N.H.**, **Harries, P.J.**, **Weinreb, D.**, **Turekian, K.K.**, **Beck, A.J.** and **Cobban, W.A.** (2010) Effect of diagenesis on the Sr, O, and C isotope

composition of late Cretaceous mollusks from the western interior seaway of North America. Am. J. Sci., **310**, 69–88.

Dauphin, Y., Williams, C.T. and Barskov, I.S. (2007) Aragonitic rostra of the Turonian belemnitid *Goniocamax*: arguments from diagenesis. Acta Palaeontol. Pol., **52**, 85–97.

Dietzel, M., Gussone, N. and Eisenhauer, A. (2003) Co-precipitation of $Sr^{2+}$ and $Ba^{2+}$ with aragonite by membrane diffusion of $CO_2$ between 10 and 50°C. Chem. Geol., **203**, 139–151.

Dodd, R.D. (1965) Environmental control of strontium and magnesium in *Mytilus*. Geochim. Cosmochim. Acta, **29**, 385–398.

Dutton, A., Lohmann, K.C. and Zinsmeister, W.J. (2002) Stable isotope and minor elements proxies for Eocene climate of Seymour Island, Antarctica. Palaeoceanography, **17**, 1016.

Elderfield, H. and Gieskes, J.M. (1982) Sr isotopes in interstitial waters of Deep Sea Drilling Project cores. Nature, **300**, 493–497.

Elliot, M.B., deMenocal, B.K.L. and Howe, S.S. (2003) Environmental controls on the stable isotopic composition of *Mercenaria mercenaria*. Potential application to paleoenvironmental studies. Geochem. Geophys. Geosyst., **4**, 1056.

Elliot, M., Welsh, K., Chicott, C., McCulloch, M., Chappell, J. and Ayling, B. (2009) Profiles of trace elements and stable isotopes derived from giant long-lived *Tridacta gigas* bivalves: potential applications in paleoclimate studies. Palaeogeogr. Palaeoclimatol. Palaeoecol., **280**, 132–142.

Epstein, S., Buchsbaum, R., Lowenstam, H.A. and Urey, H.C. (1953) Revised carbonate-water isotopic temperature scale. Geol. Soc. Am. Bull., **64**, 1316–1326.

Faure, G. and Mensing, T. (2005) Isotopes. Principles and Applications. John Wiley & Sons, New Jersey, 897 pp.

Fielding, C.G., Atkins, C.B., Basset, K.N., Browne, G.H., Dunbar, G.B., Field, B.D., Frank, T.D., Krissek, L.A., Panter, K.S., Passchier, S., Pekar, S.F., Sandroni, S. and Talarico, F. (2008) Sedimentology and stratigraphy of the AND-2A core, ANDRILL Southern McMurdo Sound Project, Antarctica. In: Studies from the ANDRILL, Southern McMurdo Sound Project, Antarctica (Eds D.M. Harwood, F. Florindo, F. Talarico and R.H. Levy), Terra Antarct., 15, 77–112.

Folk, R. (1965) Some aspects of recrystallization in ancient limestones. SEPM Spec. Publ., **13**, 14–48.

Foster, L.C., Allison, N., Finch, A.A. and Anderson, C. (2009) Strontium distribution in the shell of the aragonite bivalve *Arctica islandica*. Geochem. Geophys. Geosyst., **10**, Q03003, doi:10.1029/2007GC001915.

Frank, T.D., Gui, Z. and the ANDRILL SMS Science Team (2010) Cryogenic origin for brine in the subsurface of southern McMurdo Sound, Antarctica. Geology, **38**, 587–590.

Freitas, P.S., Clarke, L.J., Kennedy, H., Richardson, C.A. and Abrantes, F. (2006) Environmental and biological controls on elemental (Mg/Ca, Sr/Ca and Mn/Ca) ratios in shells of the king scallop *Pecten maximus*. Geochim. Cosmochim. Acta, **70**, 5119–5133.

Gaetani, G.A. and Cohen, A.L. (2006) Element partitioning during precipitation of aragonite from seawater: a framework for understanding paleoproxies. Geochim. Cosmochim. Acta, **70**, 4617–4634.

Gillikin, D.P., Lorrain, A., Navez, J., Taylor, J.W., André, L., Keppens, E., Baeyens, W. and Dehairs, F. (2005) Strong biological controls on Sr/Ca rations in aragonitic marine bivalve shells. Geochem. Geophys. Geosyst., **6**, Q05009, doi:10.1029/2004GC000874.

Gonzalez, L. and Lohmann, K.C. (1985) Carbon and oxygen isotopic composition of Holocene reefal carbonates. Geology, **13**, 811–814.

Graustein, W.C. (1989) $^{87}Sr/^{86}Sr$ ratios measure the sources and flow of strontium in terrestrial ecosystems. In: Ecological Studies (Eds P.W. Rundel, J.R. Ehleringer and K.A. Nagy), **68**, 491–512.

Grossman, E.L. and Ku, T.-L. (1986) Oxygen and carbon isotope fractionation in biogenic aragonite; temperature effects. Chem. Geol., **59**, 59–74.

Gui, Z. (2009) Origin of brines in Neogene sediments of the Ross Sea, Antarctica: AND-2A Core, ANDRILL, Southern McMurdo Sound Project. MS Thesis. University of Nebraska, Lincoln, 51 pp.

Hart, S.R. and Blusztajn, J. (1998) Clams as recorders of ocean ridge volcanism and hydrothermal vent field activity. Science, **280**, 883–886.

Harwood, D.M., Florindo, F., Levy, R.H., Fielding, C.G., Pekar, S.F. and Speece, M.A. (2005) ANDRILL Southern McMurdo Sound Project Scientific Prospectus. ANDRILL SMO Contribution No. 5, Lincoln, 29 p.

Harwood, D.M., Levy, R.H., Cowie, J., Florindo, F., Naish, T., Powell, R. and Pyne, A. (2006) Deep drilling with the ANDRILL program in Antarctica. Sci. Drilling, **3**, 43–45.

Harwood, D.M., Florindo, F., Talarico, F., Levy, R.H., Kuhn, G., Naish, T., Niessen, F., Powell, R., Pyne, A. and Wilson, G.S. (2009) Antarctic drilling recovers stratigraphic records from the continental margin. EOS Trans. Am. Geophys. Union, **90**, 90–91.

Hess, J., Bender, M. and Schilling, J.-G. (1986) Evolution of the ratio of strontium-87 to strontium-86 in seawater from cretaceous to present. Science, **231**, 979–984.

Hoefs, J. (1997) Stable Isotope Geochemistry. Springer, Berlin, 201 pp.

Howarth, R.J. and McArthur, J.M. (1997) Statistics for strontium isotope stratigraphy. A robust LOWESS fit to marine Sr-isotope curve for 0–206 Ma, with look-up tables for the derivation of numerical age. J. Geol., **105**, 441–456.

Ingram, B.L. and Depaolo, D.J. (1993) A 4300-year strontium isotope record of estuarine palaeosalinity in San-Francisco Bay, California. Earth Planet. Sci. Lett., **119**, 103–119.

**Israelson, C.** and **Buchardt, B.** (1999) Strontium and oxygen isotopic composition of East Greenland rivers and surface waters: implication for palaeoenvironmental interpretation. Palaeogeogr. Palaeoclimatol. Palaeoecol., **153**, 93–104.

**Kashiwagi, H.**, **Ogawa, Y.** and **Shikazono, N.** (2008) Relationship between weathering, mountain uplift, and climate during the Cenozoic as deduced from the global carbon-strontium cycle model. Palaeogeogr. Palaeoclimatol. Palaeoecol., **270**, 139–149.

**Kim, S.-T.**, **O'Neil, J.R.**, **Hillaire-Marcel, C.** and **Mucci, A.** (2007) Oxygen isotope fractionation between synthetic aragonite and water: influence of temperature and $Mg^{2+}$ concentration. Geochim. Cosmochim. Acta, **71**, 4704–4715.

**Kinsman, D.** (1969) Interpretations of $Sr^{2+}$ concentrations in carbonate minerals and rocks. J. Sed. Petrol., **39**, 486–508.

**Kinsman, D.** and **Holland, H.D.** (1969) The co-precipitations of cations with $CaCO_3$ – IV. The co-precipitation of $Sr^{2+}$ with aragonite between 16° and 96°C. Geochim. Cosmochim. Acta, **33**, 1–17.

**Lavelle, M.** (1998) Strontium-isotope stratigraphy of the CRP-1 drillhole, Ross Sea, Antarctica. Terra Antarct., **5**, 691–696.

**Lavelle, M.** (2000) Strontium isotope stratigraphy and age model for CRP-2/2A, Victoria Land Basin, Antarctica. Terra Antarct., **7**, 611–619.

**Lavelle, M.** (2001) Strontium isotope stratigraphy for CRP-3, Victoria Land Basin, Antarctica. Terra Antarct., **8**, 593–597.

**Li, G.J.**, **Chen, J.**, **Ji, J.**, **Liu, L.**, **Yang, J.** and **Sheng, X.** (2007) Global cooling forced increase in marine strontium isotopic ratios: importance of mica weathering and a kinetic approach. Earth Planet. Sci. Lett., **254**, 303–312.

**Maliva, R.G.**, **Missimer, T.M.** and **Dickson, J.A.D.** (2000) Skeletal aragonite neomorphism in Plio-Pleistocene sandy limestones and sandstones, Hollywood, Florida, USA. Sed. Geol., **136**, 147–154.

**Mann, R.**, **Gieskes J.M.** (1975) Interstitial waters studies, Leg 28. In: Initial Reports of the Deep Sea Drilling Project (Eds D. E. Hayes, L.A. Frakes, P.J. Barrett, D.A. Burns, P.-H. Chen, A.B. Ford, A.G. Kaneps, E. M. Kemp, D.W. McCollum, D.J. W. Piper, R. E. Wall, and P.N. Webb), **28**, 805–814.

**Marcano, M.C.**, **Mukasa, S.**, **Lohmann, K.C.**, **Stefano, C.**, **Taviani, M.** and **Andronikov, A.** (2009) Chronostratigraphic and paleoenvironmental constraints derived from the $^{87}Sr/^{86}Sr$ and $\delta^{18}O$ signal of Miocene bivalves, Southern McMurdo Sound, Antarctica. Global Planet. Change, **69**, 124–132.

**McArthur, J.M.**, **Howarth, R.J.** and **Bailey, T.R.** (2001) Strontium isotope stratigraphy: LOWESS Version 3. Best-fit line to the marine Sr-isotope curve for 0 to 509 Ma and accompanying look-up table for deriving numerical age. Look-up table Version 4:08/04. J. Geol., **109**, 155–169.

**McConnaughey, T.** (1989a) $^{13}C$ and $^{18}O$ isotopic disequilibrium in biological carbonates: I. Patterns. Geochim. Cosmochim. Acta, **53**, 151–162.

**McConnaughey, T.** (1989b) $^{13}C$ and $^{18}O$ isotopic disequilibrium in biological carbonates: II. In vitro simulation of kinetic isotope effects. Geochim. Cosmochim. Acta, **53**, 163–171.

**McConnaughey, T.** and **Gillikin, D.P.** (2008) Carbon isotopes in mollusks shell carbonates. Geo-Mar. Lett., **28**, 287–299.

**Moore, R.C.** (1969) Treatise on invertebrate paleontology. Part N. Mollusca 6 Bivalvia, Vols 1, 2. No. 3. The Geological Society of America, Laurence, 951 pp.

**Morse, J.W.** and **MacKenzie, F.T.** (1990) Geochemistry of Sedimentary Carbonates. Elsevier, Amsterdam, 707 pp.

**Mukasa, S.B.**, **Shervais, J.W.**, **Wilshier, H.G.** and **Nielson, J.E.** (1991) Intrinsic Nd, Pb, and Sr isotopic heterogeneities exhibited by the Lherz Peridotite massif, French Pyrenees. J. Petrol., Special Volume **2**, 117–134.

**Naish, T.R.**, **Powell, R.**, **Levy, R.H.**, **Henrys, S.**, **Krissek, L.A.**, **Niessen, F.**, **Pompilio, M.**, **Scherer, R.**, **Wilson, G.S.** and **Team, t.A.-M.S.** (2007) Synthesis of the initial scientific results of the MIS project (AND-1B core), Victoria Land Basin, Antarctica. Terra Antarct., **14**, 317–327.

**Naish, T.R.**, **Wilson, G.S.**, **Dunbar, G.B.** and **Barrett, P.J.** (2008) Constraining the amplitude of Late Oligocene bathymetric changes in western Ross Sea during orbitally-induced oscillation in the East Antarctic Ice Sheet: (2) implication for global sea-level changes. Palaeogeogr. Palaeoclimatol. Palaeoecol., **260**, 66–76.

**Panter, K.S.**, **Talarico, F.**, **Basset, K.N.**, **Del Carlo, P.**, **Field, B.D.**, **Frank, T.D.**, **Hoffmann, S.**, **Kuhn, G.**, **Sandroni, S.**, **Taviani, M.**, **Bracciali, L.**, **Cornamusini, G.**, **von Eynatten, H.**, **Rocchi, S.** and **Team, t.A.-S.S.** (2008) Petrology and geochemistry of the AND-2A core, ANDRILL Southern McMurdo Sound Project, Antarctica. In: Studies from the ANDRILL, Southern McMurdo Sound Project, Antarctica (Eds D.M. Harwood, F. Florindo, F. Talarico and R.H. Levy), Terra Antarct., **15**, 147–192.

**Sessa, J.A.**, **Ivany, L.C.**, **Schlossnagle, T.H.**, **Samson, S.D.** and **Schellenberg, S.A.** (2012) The fidelity of oxygen and strontium isotope values from shallow shelf settings: implications for temperature and age reconstructions. Palaeogeogr. Palaeoclimatol. Palaeoecol., **342**, 27–39.

**Shirai, K.**, **Schöne, B.R.**, **Miyaji, T.**, **Radarmacher, P.**, **Krause, R.A., Jr** and **Tanabe, K.** (2014) Assessment of the mechanism of elemental incorporation into bivalve shells (*Arctica islandica)* based on elemental distribution at the microstructural scale. Geochim. Cosmochim. Acta, **126**, 307–320.

**Smalley, C.**, **Higgins, A.C.**, **Howarth, R.J.**, **Nicholson, H.**, **Jones, C.E.**, **Swinburne, N.H.M.** and **Bessa, J.** (1994) Seawater Sr isotope variations through time: a procedure for constructing a reference curve to date and correlate marine sedimentary rocks. Geology, **22**, 431–434.

**Stecher, H.A.**, **Krantz, D.E.**, **Lord, C.J.**, **Luther, G.W.** and **Bock, K.W.** (1996) Profiles of strontium and barium in

*Mercenaria mercenaria* and *Spisula solidissima* shells. Geochim. Cosmochim. Acta, **60**, 3445–3456.

**Stipp, S.L.S.**, **Hochella, M.F., Jr**, **Parks, G.A.** and **Leckie, J.O.** (1992) Cd$^{+2}$ uptake by calcite, solid-state diffusion, and the formation of solid-solution: interface processes observed with near-surface sensitive techniques (XPS, LEED, and AES). Geochim. Cosmochim. Acta, **56**, 1941–1954.

**Stipp, S.L.S.**, **Konnerup-Madsen, J.**, **Franzreb, K.**, **Kulik, A.** and **Mathieu, H.J.** (1998) Spontaneous movement of ions through calcite at standard temperature and pressure. Nature, **396**, 356–359.

**Surge, D.** and **Walker, K.J.** (2006) Geochemical variation in microstructural shell layers of the southern quahog (*Mercenaria campechiensis*): implications for reconstructing seasonality. Palaeogeogr. Palaeoclimatol. Palaeoecol., **237**, 182–190.

**Takesue, R.K.**, **Bacon, C.R.** and **Thompson, J.K.** (2008) Influences of organic matter and calcification rate on trace elements in aragonitic estuarine bivalves shells. Geochim. Cosmochim. Acta, **72**, 5431–5445.

**Taviani, M.**, **Hannah, M.**, **Harwood, D.M.**, **Ishman, S.E.**, **Johnson, K.**, **Olney, M.**, **Riesselman, C.**, **Tuzzi, E.**, **Beu, A.G.**, **Blair, S.**, **Cantarelli, V.**, **Ceregato, A.**, **Corrado, S.**, **Mohr, B.**, **Nielson, S.H.H.**, **Persico, D.**, **Petrushak, S.**, **Raine, J.I.**, **Warny, S.** and the ANDRILL-SMS Science Team (2009) Palaeontological characterisation and analysis of the AND-2A core, ANDRILL Southern McMurdo Sound Project, Antarctica. Terra Antarct., **15**, 113–146.

**Thierstein, H.R.**, **MacDougall, J.D.**, **Martin, E.E.**, **Larsen, B.**, **Barron, J.A.** and **Baldauf, J.** (1991) Age determinations of Paleogene diamictites from Prydz Bay (Site 739), Antarctica, using Sr isotopes of mollusks and biostratigraphy of microfossils (diatoms and coccoliths). In: Proceedings of the Ocean Drilling Program, Scientific Results (Eds J. Barron, B. Larsen, J.Q. Baldauf, C. Alibert, S. Berkowitz, J.-P. Caulet, S. Chambers, A. Cooper, R. Cranston, W. Dorn, W. Ehrmann, R. Fox, G. Fryxell, M. Hambrey, B. Huber, C. Jenkins, S.-H. Kang, B. Keating, K. Mehl, I.I. Noh , Q. Oilier, A. Pittenger, H. Sakai, C. Schroder, A. Solheim, D. Stockwell, H. Thierstein, B. Tocher, B. Turner, and W. Wei), **119**, 742–745.

**Veizer, J.** (1983) Trace elements and isotopes in sedimentary carbonates. Rev. Mineral., **11**, 265–299.

**Wada, H.** and **Okada, H.** (1989) Carbonate isotopes. In: Antarctic Cenozoic History from the CIROS-1 Drillhole, McMurdo Sound, Antarctica (Ed. P.J. Barrett), DSIR, **245**, 195–200.

**Walter, L.M.** (1986) Relative efficiency of carbonate dissolution and precipitation during diagenesis, a progress report of the role of solution chemistry. In: Special Publication Society of Economic Paleontologists and Mineralogists (Ed. D.L. Gautier), SEPM Spec. Publ., **38**, 1–11.

**Walter, L.M.** and **Morse, J.W.** (1985) The dissolution kinetics of shallow marine carbonates in seawater: a laboratory study. Geochim. Cosmochim. Acta, **49**, 1503–1513.

**Wierzbowski, H.**, **Anczkiewicz, R.**, **Bazarnik, J.** and **Pawlak, J.** (2012) Strontium isotope variations in Middle Jurassic (Labe Bajocian-Callovian) seawater: implications for Earth's tectonic activity and marine environments. Chem. Geol., **334**, 171–181.

**Wilson, G.S.**, **Levy, R.H.**, **Browne, G.H.**, **Cody, R.**, **Dunbar, N.**, **Florindo, F.**, **Henrys, S.**, **Graham, I.**, **McIntosh, W.C.**, **McKay, R.M.**, **Naish, T.**, **Ohneiser, C.**, **Powell, R.**, **Ross, J.**, **Sagnotti, L.**, **Scherer, R.**, **Sjunneskog, C.**, **Strong, C.P.**, **Taviani, M.**, **Winter, D.** and **Team, t.A.-M.S.** (2007) Preliminary integrated chronostratigraphy of the AND-1B core, ANDRILL McMurdo Ice Shelf Project, Antarctica. Terra Antarct., **14**, 297–316.

**Wonik, T.**, **Grelle, T.**, **Hardwerger, D.**, **Jarrard, R.D.**, **McKee, A.**, **Patterson, T.**, **Paulsen, T.**, **Pierdominici, S.**, **Schmitt, D.R.**, **Schroder, H.**, **Speece, M.A.**, **Wilson, T.** and **Team, t.A.-S.S.** (2008) Downhole measurements in the AND-2A borehole, ANDRILL Southern McMurdo Sound Project, Antarctica. In: Studies from the ANDRILL, Southern McMurdo Sound Project, Antarctica (Eds D.M. Harwood, F. Florindo, F. Talarico and R.H. Levy), Terra Antarct., **15**, 57–68.

## Supporting Information

Additional Supporting Information may be found in the online version of this article:

**Appendix S1.** Diagram of the sample mounting and the orientation angles described for analyses on the Rigaku R-Axis Spider diffractometer.

**Appendix S2.** EPMA determined Sr concentration in aragonite fragment.

**Appendix S3.** Cathodoluminescence and reflected light images of selected venerid fragments recovered from ANDRILL core AND-2A.